

Spawning and merging of Fourier modes and phase coupling in cosmological density bispectrum

Lung-Yih Chiang[★]

Theoretical Astrophysics Center, Juliane Maries Vej 30, DK-2100, Copenhagen, Denmark

Accepted 2003 ???? ???; Received 2003 ???? ???

ABSTRACT

In the standard picture of cosmological structure formation, initially random-phase fluctuations are amplified by non-linear gravitational instability to produce a final distribution of mass which is highly non-Gaussian and has highly-coupled Fourier phases. We use the Zel'dovich approximation in one dimension to elucidate the onset of non-linearity including mode spawning, merging and coupling. We show that as gravitational clustering proceeds, Fourier modes are spawned from parent ones, with their phases following a harmonic relationship with the wavenumbers. Spawned modes could also merge leading to modulation of the amplitudes and phases which consequently breaks such harmonic relation. We also use simple toy models to demonstrate that bispectrum, Fourier transform of connected three-point correlation functions, measures phase coupling at most at the second-order only when the special wavenumber-phase harmonic relation holds. Phase information is therefore partly registered in bispectrum and it takes a complete hierarchy of polyspectra to fully characterize gravitational non-linearity.

Key words: cosmology : theory – large-scale structure of the Universe – techniques: analytical

1 INTRODUCTION

One of the main issues in cosmology is quantitative characterization of the large-scale structure of the Universe. The Universe from present observations is highly non-linear on scales up to roughly $8h^{-1}\text{Mpc}$. In the framework of the inflation paradigm, the structure we see today is blown up from tiny inhomogeneities originated from quantum fluctuations. The cosmic microwave background has provided a strong evidence that the Universe was fairly homogeneous and isotropic with fluctuations one part in 10^5 in the past. Such initial density fluctuations in the simplest inflationary universe constitute a Gaussian random field.

Gaussian random Fields (Bardeen et al. 1986) are useful because of its analytical simplicity. One particularly interesting property of Gaussian random fields is that the real and imaginary part of the Fourier modes are both Gaussian distributed and mutually independent, or in other words, the Fourier phases are randomly distributed between 0 and 2π . The statistical properties are then completely specified by its second-order statistics: its two-point correlation function $\xi(r)$ (with zero connected n -point correlation functions for $n > 2$), or alternatively, its power spectrum $P(k)$.

In the framework of gravitational instability, a perturbative method can be adopted at the early stage of density clustering (see e.g. Peebles 1980, Bernardeau et al. 2002). The linear perturbation theory is applicable when the density fluctuations are small i.e. its variance of density contrast $\langle \delta^2 \rangle < 1$. The statistical distribution of the density field such as originally random phases remains invariant in the linear regime, except its variance increasing with time.

The departure of the density field from the linear regime gives rise to phase coupling. Second-order statistics, such as power spectrum and two-point correlation function, throw away the fine details of the delicate pattern of cosmic structure. These details lie in the distribution of Fourier phases to which second-order statistics are blind. The evident shortcomings of $P(k)$ can be partly ameliorated by defining higher-order quantities such as the bispectrum (Peebles 1980; Goroff, Grinstein, Rey & Wise 1986; Bernardeau 1992; Hivon et al. 1995; Matarrese, Verde & Heavens 1997; Scoccimarro 1997; Scoccimarro

[★] E-mail : chiang@tac.dk

et al. 1998; Scoccimarro, Couchman & Frieman 1999; Verde et al. 2000) or correlations of $\delta(\mathbf{k})^2$ (Stirling & Peacock 1996). Higher-order correlations and polyspectra find this information term by term so that an infinite hierarchy is required for a complete statistical characterization of the fluctuation field.

Due to the close connection between morphology and Fourier phases (Chiang 2001), there have been attempts in investigating the behaviour of phases (Ryden & Gramann 1991; Soda & Suto 1992; Jain & Bertschinger 1998). They focus on phase shift from the original one. Scherrer, Melott and Shandarin (1991) develop a practical method on quantifying phase coupling. Chiang & Coles (2000) take phase difference between neighbouring modes on Shannon entropy to quantify phase information. Due to the circular nature of phases, a novel visualization method is also developed (Coles & Chiang 2000). Chiang, Coles & Naselsky (2002) and Chiang, Naselsky & Coles (2002) develop a novel method, return mapping of phases to render phases onto a ‘return map’ to quantify phase associations between different $\Delta\mathbf{k}$. Watts, Coles & Melott (2003) have shown that the probability distribution of phase difference between neighbouring modes displays a universal behaviour for clustering phenomenon.

Since both Fourier phase coupling and non-zero higher-order correlation functions depict gravitational non-linearity, Watts & Coles (2002); Matsubara (Matsubara 2003) have shown the relationships between phase coupling and bispectrum which displays the lowest order non-linearity in density perturbations. Hikage, Matsubara & Suto (2003) have used phase sum from wavenumbers (\mathbf{k} vectors) forming a triangle as a descriptor of non-linear gravitational clustering.

Despite the progress described above, efforts are yet to be made in understanding the direct relationship between gravitational clustering and phase coupling. In this paper we use one-dimensional Zel’dovich approximation as a clustering scheme to investigate mode coupling when gravitational perturbations depart from the linear regime. This moment is related to the so-called *quadratic density fields* (Coles & Barrow 1987; Watts & Coles 2002 and references therein), in which the quadratic term induces non-linearity. The non-linearity caused by gravitational clustering can be described in two effects: *mode spawning* by the quadratic and higher-order terms and *mode merging* leading to modulation of the amplitudes and phases. These two effects are in action as cosmological density clustering proceeds.

This paper is organized as follows. In Section 2 we re-visit some useful technical background: the commonly-used statistical tools and theories: the power spectrum and two-point covariance functions, the linear theory of cosmological density perturbations, and the Zel’dovich approximation which in one dimension provides the insight on phase coupling. In Section 3 we use such one-dimensional model as a clustering scheme for analyses of the onset of the following phenomena: mode spawning and merging from gravitational clustering and their relationships with bispectrum. We further examine these phenomena by direct 1D simulations into highly non-linear regime in Section 4. The discussions are in Section 5. For completeness in the Appendix we prove the exactness of the density evolution from the 1D Zel’dovich approximation.

2 TECHNICAL BACKGROUND

2.1 Power spectrum and two-point covariance functions

The mathematical description of an inhomogeneous Universe revolves around the dimensionless density contrast, $\delta(\mathbf{x})$, which is obtained from the spatially-varying matter density $\rho(\mathbf{x})$ via

$$\delta(\mathbf{x}) = \frac{\rho(\mathbf{x}) - \rho_0}{\rho_0}, \quad (1)$$

where \mathbf{x} is the comoving coordinate, ρ_0 is the global mean density (Peebles 1980). The two-point covariance function, which measures the excess probability over Poisson distribution between a pair with separation \mathbf{r} , is defined as

$$\xi(\mathbf{r}) = \langle \delta(\mathbf{x})\delta(\mathbf{x} + \mathbf{r}) \rangle, \quad (2)$$

where the mean is taken over all points \mathbf{x} . It is also useful to expand the density contrast in Fourier series, in which δ is treated as a superposition of plane waves:

$$\delta(\mathbf{x}) = \sum \delta(\mathbf{k}) \exp(i\mathbf{k} \cdot \mathbf{x}). \quad (3)$$

The Fourier transform $\delta(\mathbf{k})$ is complex and therefore possesses both amplitude $|\delta(\mathbf{k})|$ and phase $\phi_{\mathbf{k}}$ where

$$\delta(\mathbf{k}) = |\delta(\mathbf{k})| \exp(i\phi_{\mathbf{k}}). \quad (4)$$

The power spectrum is defined as

$$\langle \delta(\mathbf{k}_1)\delta(\mathbf{k}_2) \rangle = (2\pi)^3 P(k) \delta^D(\mathbf{k}_1 + \mathbf{k}_2), \quad (5)$$

which is the Fourier transform of the two-point covariance function via Wiener-Khintchin theorem. We can analogously define the bispectrum as the third-order moment in Fourier space:

$$\langle \delta(\mathbf{k}_1)\delta(\mathbf{k}_2)\delta(\mathbf{k}_3) \rangle = (2\pi)^3 B(\mathbf{k}_1, \mathbf{k}_2, \mathbf{k}_3) \delta^D(\mathbf{k}_1 + \mathbf{k}_2 + \mathbf{k}_3), \quad (6)$$

which is the Fourier transform of the connected three-point covariance function.

2.2 The linear theory of density perturbations

Gravitational instabilities is believed to be the driving force of large-scale structure formation. When the density perturbation is small, evolution of the density contrast can be obtained analytically through the *linear perturbation theory* from 3 coupled partial differential equations. They are the linearized continuity equation,

$$\frac{\partial \delta}{\partial t} = -\frac{1}{a} \nabla_x \cdot \mathbf{v}, \quad (7)$$

the linearized Euler equation

$$\frac{\partial \mathbf{v}}{\partial t} + \frac{\dot{a}}{a} \mathbf{v} = -\frac{1}{\rho a} \nabla_x p - \frac{1}{a} \nabla_x \phi, \quad (8)$$

and the linearized Poisson equation

$$\nabla_x^2 \phi = 4\pi G a^2 \rho_0 \delta. \quad (9)$$

In these equations, a is the expansion factor, p is the pressure, ∇_x denotes a derivative with respect to the comoving coordinates \mathbf{x} , $\mathbf{v} = a\dot{\mathbf{x}}$ is the peculiar velocity and $\phi(\mathbf{x}, t)$ is the peculiar gravitational potential. From Eq.(7)-(9), and if one ignores pressure forces, it is easy to obtain an equation for the evolution of δ :

$$\ddot{\delta} + 2\left(\frac{\dot{a}}{a}\right)\dot{\delta} - 4\pi G \rho_0 \delta = 0. \quad (10)$$

For a spatially flat universe dominated by pressureless matter, $\rho_0(t) = 1/6\pi G t^2$ and Eq.(10) admits two linearly independent power-law solutions

$$\delta(\mathbf{x}, t) = b_{\pm}(t)\delta_0(\mathbf{x}), \quad (11)$$

where $\delta_0(\mathbf{x})$ is the initial density distribution, $b_+(t) \propto a(t) \propto t^{2/3}$ is the growing mode and $b_-(t) \propto t^{-1}$ is the decaying mode.

As one can see from Eq.(11), the growth depends only on time, so the growth of density distribution in the linear regime does not alter the phases.

2.3 The Zel'dovich Approximation

In order to examine analytically non-linear effects induced by gravitational clustering, we use the Zel'dovich approximation (1970) as a clustering scheme, which extrapolates the evolution of density perturbations into non-linear regime. This extrapolation from the linear theory follows the perturbation in particle trajectories rather than in density fields. In the Zel'dovich approximation (ZA), a particle initially placed at the Lagrangian coordinate \mathbf{q} is perturbed after a time t to an Eulerian coordinate \mathbf{x} . The displacement of the particle simply depends on the constant velocity the particle has when it is kicked off its initial position, and can be written as $b(t)\mathbf{u}(\mathbf{q})$, so that

$$\mathbf{r}(\mathbf{q}, t) = a(t)\mathbf{x}(\mathbf{q}, t) = a(t)[\mathbf{q} + b(t)\mathbf{u}(\mathbf{q})], \quad (12)$$

where \mathbf{r} is the resultant physical coordinate, $a(t)$ is the expansion factor and $b(t)$ is the growing mode $b_+(t)$ from the linear perturbation theory. According to this prescription, each particle moves with a constant velocity along a ballistic trajectory, which resembles Newtonian inertial motion. Note that the peculiar velocity according to the ZA is $a\dot{\mathbf{x}} = a(t)\dot{b}(t)\mathbf{u}(\mathbf{q})$. For an irrotational flow, $\mathbf{u}(\mathbf{q})$ can be expressed as a gradient of some velocity potential $-\nabla\Phi_0(\mathbf{q})$.

We focus particularly on the applications of one-dimensional ZA. The ZA in 1D provides an exact solution of density evolution (Buchert 1992) in that the evolution of planar collapse from the ZA has the same solution as from the Poisson equation until shell-crossing (Padmanabhan 1993). The ZA in 1D is simplified to

$$x(q, t) = q + b(t)u(q) = q - b(t)\frac{d\Phi_0(q)}{dq}. \quad (13)$$

The density contrast can be derived from the conservation of mass $\rho dx = \rho_0 dq$:

$$\delta = \frac{\rho}{\rho_0} - 1 = \left(\frac{\partial x}{\partial q}\right)^{-1} - 1 = \left[1 - b(t)\frac{d^2\Phi_0(q)}{dq^2}\right]^{-1} - 1 \quad (14)$$

$$= \sum_n b^n(t) \left(\frac{d^2\Phi_0}{dq^2}\right)^n. \quad (15)$$

The velocity potential $\Phi_0(q)$ can always be disintegrated as

$$\Phi_0(q) = \sum_i A_i \cos(\lambda_i q + \alpha_i). \quad (16)$$

One can recover the solution to the linear theory from Eq.(14) by taking partial differentiation $\partial/\partial t$ on both sides. Substituting $d^2\Phi_0/dq^2$ with $b^{-1}\delta/(\delta+1)$, we reach

$$\frac{\partial\delta}{\partial t} = \frac{\dot{b}}{b}(\delta + \delta^2). \quad (17)$$

Equation (17) provides us the insight into phase coupling from gravitational clustering. One important property of Eq.(17) is that the δ^2 term is the “culprit” of the onset of non-linearity. Without the δ^2 term we obtain the same solution as that from the linear theory, $\delta \propto b$ ($\propto t^{2/3}$ if the Universe is matter-dominated), i.e. density fields grow only with time in the linear regime where the phases are unchanged (and uncorrelated if primordial Gaussianity is assumed). It is this quadratic term δ^2 that the density field breaks away from the linear regime and produces gravitational non-linearity, hence phase coupling. In Eq.(17), the quadratic term δ^2 is related to the “quadratic density field” (Coles & Barrow 1987; Watts & Coles 2002).

3 MODE COUPLING AND BISPECTRUM

In this section we use 1D ZA to demonstrate spawning and merging of Fourier modes and phase coupling induced by gravitational clustering and its relation with bispectrum. For the analyses in this Section, we consider only an early stage of evolution, i.e. $b(t) \ll 1$ and assume that the curvature of the velocity potential is small such that $x \simeq q$ and $dx \simeq dq$. Fourier transform can then be performed in the Lagrangian coordinate q . Direct simulations of 1D ZA for gravitational evolution is in Section 4.

3.1 Mode spawning and mode merging

Upon using 1D ZA, we firstly choose as a toy model the velocity potential [†]

$$\Phi_0(q) = -A_1 \cos(\lambda_1 q + \alpha_1) - A_2 \cos(\lambda_2 q + \alpha_2). \quad (18)$$

When $b(t) \ll 1$, the density contrast can be expressed in terms of only the first order from Eq.(15)

$$\delta \simeq \delta^{(1)} = b(t) \left(\frac{d^2\Phi_0}{dq^2} \right) = a_1 \cos(\lambda_1 q + \alpha_1) + a_2 \cos(\lambda_2 q + \alpha_2) \equiv a_1 \begin{pmatrix} \lambda_1 \\ \alpha_1 \end{pmatrix} + a_2 \begin{pmatrix} \lambda_2 \\ \alpha_2 \end{pmatrix}, \quad (19)$$

where the round brackets hereafter denote cosine functions, $a_1 = b(t)A_1\lambda_1^2$ and $a_2 = b(t)A_2\lambda_2^2$. After Fourier transform in Lagrangian coordinate we have only two modes with wavenumbers λ_1 and λ_2 , and phases α_1 and α_2 , respectively. So these are the only Fourier modes the moment the clustering process begins (which we call the “parent modes”). It is clear that the first order does not display phase coupling. When the second-order term becomes comparable,

$$\begin{aligned} \delta &\simeq \delta^{(1)} + \delta^{(2)} = b(t) \left(\frac{d^2\Phi_0}{dq^2} \right) + b^2(t) \left(\frac{d^2\Phi_0}{dq^2} \right)^2 \\ &= \frac{a_1^2 + a_2^2}{2} + a_1 \begin{pmatrix} \lambda_1 \\ \alpha_1 \end{pmatrix} + a_2 \begin{pmatrix} \lambda_2 \\ \alpha_2 \end{pmatrix} + a_1^2 \begin{pmatrix} 2\lambda_1 \\ 2\alpha_1 \end{pmatrix} + a_2^2 \begin{pmatrix} 2\lambda_2 \\ 2\alpha_2 \end{pmatrix} + a_1 a_2 \begin{pmatrix} \lambda_1 + \lambda_2 \\ \alpha_1 + \alpha_2 \end{pmatrix} + a_1 a_2 \begin{pmatrix} \lambda_1 - \lambda_2 \\ \alpha_1 - \alpha_2 \end{pmatrix}. \end{aligned} \quad (20)$$

Since the density contrast in 1D ZA can be expressed as a power series of $d^2\Phi_0/dq^2$ in Eq. (15), the second-order term reflects the quadratic density fields (Coles & Barrow 1987; Watts & Coles 2002). This second-order term spawns modes with wavenumbers that are from combinations of any 2 wavenumbers from the parent ones, i.e. Fourier modes with wavenumbers $2\lambda_1$, $2\lambda_2$, $\lambda_1 + \lambda_2$ and $\lambda_1 - \lambda_2$ spawned from combination of λ_1 and λ_2 . One important feature of quadratic density fields is that the phases of the spawned modes follow the same kind of harmonic relationship as the spawned wavenumbers, which we call hereafter “wavenumber-phase harmonic relation”. Such relation subsequently forms phase associations between Fourier modes and is crucial for bispectrum analysis.

We can generalize the velocity potential in 1D ZA as a sum of cosine functions $\Phi_0 = -\sum_i A_i \cos(\lambda_i q + \alpha_i)$. The density contrast of the first order and that up to the second order now become, respectively,

$$\delta^{(1)} = \sum_i a_i \cos(\lambda_i + \alpha_i) \equiv \sum_i a_i \begin{pmatrix} \lambda_i \\ \alpha_i \end{pmatrix}, \quad (21)$$

where $a_i = b(t)A_i\lambda_i^2$, and

[†] We put minus sign for both cosine functions in the velocity potential to make the analytical form neat, assuming both A_1 and A_2 positive, otherwise the phases would have a shift by π .

$$\delta^{(1)} + \delta^{(2)} = \sum_i a_i \begin{pmatrix} \lambda_i \\ \alpha_i \end{pmatrix} + \sum_{jk} \frac{a_j a_k}{2} \left[\begin{pmatrix} \lambda_j - \lambda_k \\ \alpha_j - \alpha_k \end{pmatrix} + \begin{pmatrix} \lambda_j + \lambda_k \\ \alpha_j + \alpha_k \end{pmatrix} \right]. \quad (22)$$

If primordial Gaussianity is assumed, the phases α_i of the initial velocity potential are uniformly random and independently distributed between 0 and 2π . Below we categorize the effects induced by quadratic density fields.

• **Mode spawning** : In Eq.(22) beyond the first order, new modes are spawned from the $\delta^{(2)}$ and correlated phases are created following the spawned modes. The wavenumbers of the spawned modes are formed from combination of any 2 wavenumbers of the first order (the same as the toy model) and the phases follow the *wavenumber-phase harmonic relation*. Some terms may appear even at the earliest stage (when $b(t)A_j A_k (\lambda_j \lambda_k / \lambda_i)^2 > 2A_i$). Those are terms usually involving high-frequency modes, i.e. high λ_j or λ_k . Such phase coupling can manifest itself through phase mapping (Chiang, Coles & Naselsky 2002). For example, a short sequence of modes is formed with a constant difference in wavenumber $\Delta k = \lambda_k$:

$$\frac{a_j a_k}{2} \begin{pmatrix} \lambda_j - \lambda_k \\ \alpha_j - \alpha_k \end{pmatrix}, a_j \begin{pmatrix} \lambda_j \\ \alpha_j \end{pmatrix}, \frac{a_j a_k}{2} \begin{pmatrix} \lambda_j + \lambda_k \\ \alpha_j + \alpha_k \end{pmatrix}, \quad (23)$$

where the middle mode is taken from the $\delta^{(1)}$. Due to the wavenumber-phase harmonic relation, this phase sequence has a constant phase difference $\Delta\phi = \alpha_k$ and can be mapped along a line parallel to the diagonal through phase mapping technique. Such coupling between modes with large Δk is discussed in Chiang, Coles & Naselsky (2002).

• **Mode merging** : The newly-spawned modes from the second order are not all independent but could merge with modes of the same wavenumbers in the first order. Take the following two modes from Eq.(22) as an example, one from the $\delta^{(1)}$ and the other from the $\delta^{(2)}$:

$$a_i \begin{pmatrix} \lambda_i \\ \alpha_i \end{pmatrix}, \frac{a_j a_k}{2} \begin{pmatrix} \lambda_j - \lambda_k \\ \alpha_j - \alpha_k \end{pmatrix}. \quad (24)$$

If $\lambda_j - \lambda_k = \lambda_i$, i.e. the wavenumber of the newly-spawned mode coincides with the one in the first order, and when $b(t)$ reaches a stage $b(t) \simeq 2(A_i/A_j A_k)(\lambda_i/\lambda_j \lambda_k)^2$ such that $a_i \simeq a_j a_k/2$, these two modes merge to form a new mode:

$$2a_i \cos[(\alpha_j - \alpha_k - \alpha_i)/2] \begin{pmatrix} \lambda_i \\ \frac{\alpha_j - \alpha_k + \alpha_i}{2} \end{pmatrix}, \quad (25)$$

where the amplitude is modulated and the phase is shifted. Such modulation in amplitudes and phases proceeds gradually and the consequence is that the wavenumber-phase harmonic relation is broken. Thus not all spawned modes will enjoy the harmonic relation. Note that in this case the evolution can still be at very early stage $b(t) \ll 1$ as long as $\lambda_j \lambda_k / \lambda_i \gg (A_i/A_j A_k)^{1/2}$.

We can also look at the density contrast up to the third order,

$$\begin{aligned} \delta^{(1)} + \delta^{(2)} + \delta^{(3)} &= \sum_i a_i \begin{pmatrix} \lambda_i \\ \alpha_i \end{pmatrix} + \sum_{jk} \frac{a_j a_k}{2} \left[\begin{pmatrix} \lambda_j - \lambda_k \\ \alpha_j - \alpha_k \end{pmatrix} + \begin{pmatrix} \lambda_j + \lambda_k \\ \alpha_j + \alpha_k \end{pmatrix} \right] \\ &+ \sum_{lmn} \frac{a_l a_m a_n}{4} \left[\begin{pmatrix} \lambda_l + \lambda_m + \lambda_n \\ \alpha_l + \alpha_m + \alpha_n \end{pmatrix} + \begin{pmatrix} \lambda_l + \lambda_m - \lambda_n \\ \alpha_l + \alpha_m - \alpha_n \end{pmatrix} + \begin{pmatrix} \lambda_l - \lambda_m + \lambda_n \\ \alpha_l - \alpha_m + \alpha_n \end{pmatrix} \right. \\ &+ \left. \begin{pmatrix} \lambda_l - \lambda_m - \lambda_n \\ \alpha_l - \alpha_m - \alpha_n \end{pmatrix} \right]. \end{aligned} \quad (26)$$

Once again new modes are spawned, more complicated phase coupling appears and the spawned modes also merge with parent modes. We shall look at mode spawning and coupling at higher-order modes through direct simulations.

3.2 Bispectrum and quadratic phase coupling

Bispectrum is the lowest-order statistic sensitive to the structure generated by gravitational clustering (Peebles 1980). It is defined as two-dimensional Fourier transform of the connected three-point auto-covariance function ζ

$$\zeta(r_1, r_2) = \langle \delta(x) \delta(x + r_1) \delta(x + r_2) \rangle. \quad (27)$$

The bispectrum and higher-order polyspectra vanish for Gaussian random fields, but in a non-Gaussian field they may be non-zero. The usefulness of these and related quantities therefore lies in the fact that they encode some information about non-linearity and non-Gaussianity.

A certain form of phase relationship produces non-zero bispectrum. To see this, we simplify the $\delta^{(2)}$ of Eq.(20) by taking only the 2nd, 3rd and 6th term and denote it as the case I (Coles & Chiang 2001),

$$\delta_I = a_1 \begin{pmatrix} \lambda_1 \\ \alpha_1 \end{pmatrix} + a_2 \begin{pmatrix} \lambda_2 \\ \alpha_2 \end{pmatrix} + a_1 a_2 \begin{pmatrix} \lambda_1 + \lambda_2 \\ \alpha_1 + \alpha_2 \end{pmatrix}. \quad (28)$$

For comparison we introduce the case II:

$$\delta_{II} = a_1 \begin{pmatrix} \lambda_1 \\ \alpha_1 \end{pmatrix} + a_2 \begin{pmatrix} \lambda_2 \\ \alpha_2 \end{pmatrix} + a_1 a_2 \begin{pmatrix} \lambda_1 + \lambda_2 \\ \alpha_3 \end{pmatrix}, \quad (29)$$

where α_1 , α_2 and α_3 are random. The case I displays *quadratic phase coupling* whereas the case II exhibits no phase association. One can see that $\langle \delta_I \rangle = \langle \delta_{II} \rangle = 0$, and it is straightforward to show that the covariances for both cases are equal,

$$\xi_I(r) = \langle \delta_I(x) \delta_I(x+r) \rangle = \xi_{II}(r) = \frac{a_1^2}{2} \cos(\lambda_1 r) + \frac{a_2^2}{2} \cos(\lambda_2 r) + \frac{a_1^2 a_2^2}{2} \cos[(\lambda_1 + \lambda_2)r], \quad (30)$$

so are their power spectra. The above demonstrates that second-order statistics are blind to any phase associations.

The reduced three-point covariance function for the case I is

$$\begin{aligned} \zeta_I(r_1, r_2) = & \frac{a_1^2 a_2^2}{4} [\cos(\lambda_2 r_1 + \lambda_1 r_2) + \cos(\lambda_1 r_1 + \lambda_2 r_1 - \lambda_1 r_2) + \cos(\lambda_1 r_1 + \lambda_2 r_1 - \lambda_2 r_2) \\ & + \cos(\lambda_1 r_1 + \lambda_2 r_2) + \cos(\lambda_1 r_2 + \lambda_2 r_2 - \lambda_1 r_1) + \cos(\lambda_1 r_2 + \lambda_2 r_2 - \lambda_2 r_1)], \end{aligned} \quad (31)$$

and for arbitrary α_1 , α_2 and α_3 we get

$$\zeta_{II}(r_1, r_2) = 0. \quad (32)$$

One can see that the spawned modes of the second order which benefit from the wavenumber-phase harmonic relation induce non-zero ζ . The bispectrum, $B(k_1, k_2)$, the two-dimensional Fourier transform of ζ , for case II is $B_{II}(k_1, k_2) = 0$ trivially, whereas $B_I(k_1, k_2)$ consists of a single spike located somewhere in the region of (k_1, k_2) space defined by $k_2 \geq 0$, $k_1 \geq k_2$ and $k_1 + k_2 \leq \pi$. If $\lambda_1 \geq \lambda_2$ then the spike appears at $k_1 = \lambda_1$, $k_2 = \lambda_2$. Thus the bispectrum is the lowest order of polyspectra that measures the phase coupling induced by quadratic non-linearities when the wavenumber-phase harmonic relation holds. However, bispectrum is trivially zero again if such harmonic relation is broken. Note that this relation is easily broken by mode merging when a third phase is involved.

Following the same line of thought, we can extend this toy model from Eq.(26) to the case III,

$$\delta_{III} = a_1 \begin{pmatrix} \lambda_1 \\ \alpha_1 \end{pmatrix} + a_2 \begin{pmatrix} \lambda_2 \\ \alpha_2 \end{pmatrix} + a_3 \begin{pmatrix} \lambda_3 \\ \alpha_3 \end{pmatrix} + \frac{a_1 a_2 a_3}{4} \begin{pmatrix} \lambda_1 + \lambda_2 + \lambda_3 \\ \alpha_1 + \alpha_2 + \alpha_3 \end{pmatrix}, \quad (33)$$

and the case IV for comparison,

$$\delta_{IV} = a_1 \begin{pmatrix} \lambda_1 \\ \alpha_1 \end{pmatrix} + a_2 \begin{pmatrix} \lambda_2 \\ \alpha_2 \end{pmatrix} + a_3 \begin{pmatrix} \lambda_3 \\ \alpha_3 \end{pmatrix} + \frac{a_1 a_2 a_3}{4} \begin{pmatrix} \lambda_1 + \lambda_2 + \lambda_3 \\ \alpha_4 \end{pmatrix}, \quad (34)$$

where α_1 , α_2 , α_3 and α_4 are random. The bispectrum for both cases are zero, but the trispectrum, the three-dimensional Fourier transform of the reduced four-point covariance function, can pick up cubic phase coupling for case III (24 terms), whereas it is again trivially zero for case IV. The third-order term produces cubic phase coupling to which bispectrum is blind.

Therefore, bispectrum only measures phase coupling at the second-order. During density clustering, however, mode spawning will produce the bispectrum from case I, $\zeta_I(r_1, r_2)$ is not always non-zero. Mode merging breaking the wavenumber-phase harmonic relation results in zero bispectrum. The same would happen to all polyspectra.

Although we only demonstrate with 1D toy model the relationship between bispectrum and quadratic phase coupling, a full treatment of such relationship is elaborated in Watts & Coles (2002): a non-zero bispectrum can only be produced when the \mathbf{k} vectors form a triangle in k -space, wherein the same (quadratic) wavenumber-phase harmonic relation has to hold. Phase coupling is not registered only in bispectrum, but in all polyspectra.

4 SIMULATIONS

In this Section, we perform 1D ZA numerically in order to demonstrate mode spawning and coupling into highly non-linear regime. Due to limitation on integration in Lagrangian coordinate, in the previous Section we can analyze only the onset of non-linearity by assuming $b(t) \ll 1$. In the following simulations we assume the periodic boundary condition,

$$x(q + 2j\pi) = x(q). \quad (35)$$

4.1 Non-interactive and interactive parent modes in the simulations

Here we supply three different initial velocity potential functions to the simulations. We choose the velocity potential field with the following form for Fig. 1 and 2:

$$\Phi_0 = -\cos(7q + \theta) - \cos(11q + \phi), \quad (36)$$

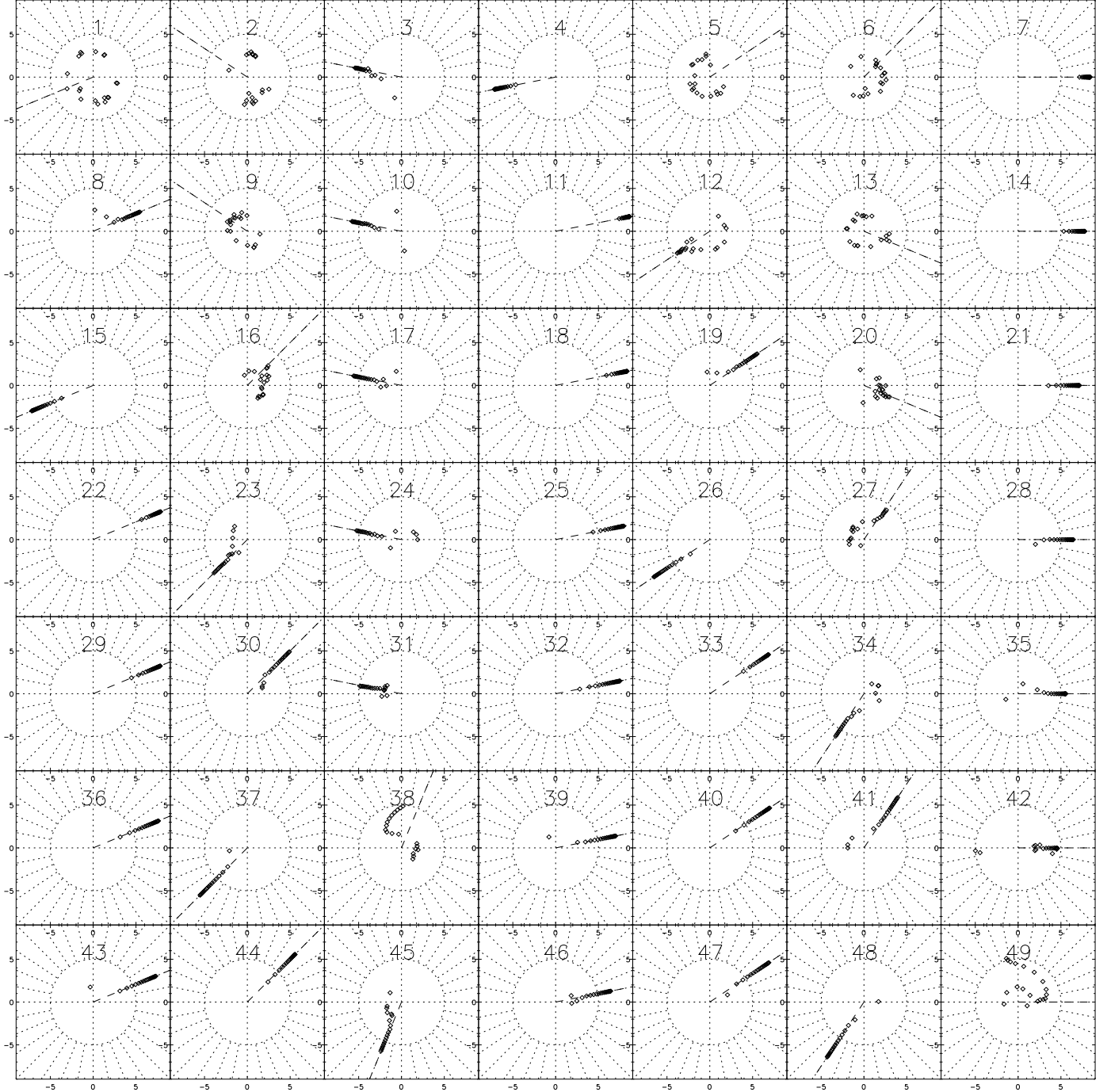


Figure 1. The amplitude and phase evolution of 1D ZA simulation with $\Phi_0 = -\cos(7q) - \cos(11q + \pi/16)$ for wavenumber $k = 1 - 49$. We specifically designate 7 small panels in one row so that in each column the increment of the wavenumber is 7. Each time step is represented by a diamond symbol. In each panel (for one Fourier mode) the amplitude ($\times 10^9$) is shown in logarithmic scale by the distance to the origin, and the phase by the angle against the positive x axis. Thus the dotted circle with radius 5 units indicates the level of amplitudes with 10^{-4} . The radial dotted lines are angles with increment of $\pi/16$ to show that phases align with angles of multiple of $\pi/16$. The dash lines are the predicted phases according to Table 1: the wavenumber-phase harmonic relation. One can see the phases of spawned modes follow this harmonic relation because they have only one primary combination from parent modes, i.e. non-interactive.

where θ and ϕ are 0 and $\pi/16$ in Fig. 1 and $\pi/4$ and $\pi/7$ in Fig. 2, respectively. As described in previous Sections, once the clustering proceeds, θ and ϕ will feed as phases of two parent modes with wavenumber 7 and 11 in these cases: α_7 and α_{11} . These specially chosen wavenumbers $\lambda_1 = 7$ and $\lambda_2 = 11$ for both Fig. 1 and 2 are “non-interactive” in the sense that the phases of spawned modes have only one primary combination from the parent ones. If the parent modes are “non-interactive”, the phases will eventually follow the harmonic relationship (see Table 1). So the phase of the spawned mode

with, for example, wavenumber $k = 25$ ($= 2 \times 7 + 11$) can only come from addition of the phases of the parent modes, in other words, $\alpha_{25} = 2 \times \alpha_7 + \alpha_{11}$.

In addition to the two simulations of “non-interactive” mode spawning, in Fig. 3 we also show the simulation with one extra “interactive” mode:

$$\Phi_0 = -\cos(7q) - \cos(11q + \pi/16) - \cos(14q + \pi/4). \quad (37)$$

Figure 3 with the extra mode $\lambda_3 = 14 = 2\lambda_1$ illustrates parent-mode interactions leading to change of phases during the clustering process. One can see now, with this extra parent mode, the spawned wavenumber $k = 25$, for example, can have two combinations: $2 \times 7 + 11$ and $11 + 14$. So the phase of this spawned mode α_{25} can now come from either $2\alpha_7 + \alpha_{11}$ or $\alpha_{11} + \alpha_{14}$.

We use the following representation in order to display simultaneously the amplitude and phase evolution for each Fourier mode. Each small panel represents one Fourier mode with denoted wavenumber. We divide the simulations (up to the shell crossing) into 20 time steps with each step represented by one diamond symbol. In each panel the amplitudes of different time steps are shown in logarithmic scale by the distances to the origin, and the phases by the angles against the positive x axis (similar to a complex-plane representation but only the magnitudes in logarithmic scale). We have to multiply all the amplitudes by 10^9 so that they are always positive after taking the logarithm[‡]. Thus the dotted circles with radius 5 units in each panel indicate a level of Fourier amplitudes 10^{-4} .

In Fig. 1 the radial dotted lines are angles with increments of $\pi/16$ to show that phases aligned with angles of multiple $\pi/16$ (which is due to combination of $\alpha_7 = 0$ and $\alpha_{11} = \pi/16$). The dash lines are the predicted phases from wavenumber-phase harmonic relation according to Table 1.

One can easily see in Fig.1 that the parent modes $k = 7$ and 11 have higher initial amplitudes than other modes for the start. We specifically designate 7 small panels in one row so that in each column the increment of the wavenumber is 7. Because wavenumber 7 is one of the parent modes, phases of the spawned modes are formed by addition of α_7 , following wavenumber-phase harmonic relation. For instance, for the wavenumbers of the Fourier modes $18 (= 11 + 7)$, $25 (= 11 + 2 \times 7)$, $32 (= 11 + 3 \times 7)$, $39 (= 11 + 4 \times 7)$, $46 (= 11 + 5 \times 7)$, their phases are formed from $\alpha_{11} + \alpha_7$, $\alpha_{11} + 2 \times \alpha_7$, $\alpha_{11} + 3 \times \alpha_7$, $\alpha_{11} + 4 \times \alpha_7$ and $\alpha_{11} + 5 \times \alpha_7$, an increment of α_7 (see Table 1 for the details of phase combination from the parent modes). It is therefore easy to see that the multiples of wavenumber 7: 7, 14, 28, 35, 42 have the same phase, as well as 8, 15, 22, 29, 36, 43. This is due to the fact that the phases formed by the increment of α_7 is unchanged when $\alpha_7 = 0$ in Fig.1. Phases of most modes eventually align with multiples of $\pi/16$ because of the following reasons: they follow the wavenumber-phase harmonic relation and the phase of one parent mode is 0. Modes with wavenumbers $k = 1, 2, 5, 6, 9$ and 13 do not align with multiples of $\pi/16$ and their amplitudes cannot reach 10^{-4} .

4.2 Analytical account for the simulations

To account for the interaction of the parent modes leading to mode merging, we can start from Eq. (14). We have

$$\delta_k = \frac{1}{2\pi} \int_{-\pi}^{\pi} \left[\left(\frac{dx}{dq} \right)^{-1} - 1 \right] e^{-ikx} dx = \frac{1}{2\pi} \int_{-\pi}^{\pi} e^{-ikx} dq = \frac{1}{2\pi} \int_{-\pi}^{\pi} \exp\{-ik[q + b(t)u(q)]\} dq, \quad (38)$$

where $u(q) = -d\Phi_0(q)/dq$. We can give the same treatment to Eq. (38) as Eq. (15) by expressing it in terms of a power series of $b(t)$:

$$\delta_k = \sum_{p=0}^{\infty} \frac{(-ikb)^p}{p!} \frac{1}{2\pi} \int_{-\pi}^{\pi} dq e^{-ikq} u(q)^p. \quad (39)$$

Following Soda & Suto (1992), we can denote the Fourier transform of $u(q)$ as u_k

$$u_k = \frac{1}{2\pi} \int_{-\pi}^{\pi} dq u(q) e^{-ikq}, \quad (40)$$

so the Fourier modes δ_k can be expressed as

$$\delta_k = -ikbu_k + \frac{(-ikb)^2}{2!} \sum_{k_1, k_2} u_{k_1} u_{k_2} \delta^D[k - (k_1 + k_2)] + \frac{(-ikb)^3}{3!} \sum_{k_1, k_2, k_3} u_{k_1} u_{k_2} u_{k_3} \delta^D[k - (k_1 + k_2 + k_3)] + \dots, \quad (41)$$

where δ^D denotes Dirac-delta function. For $u(q) = -d\Phi_0/dq = -\sum_j A_j \lambda_j \sin(\lambda_j q + \alpha_j)$ from the velocity potential $\Phi_0 = -\sum_j A_j \cos(\lambda_j q + \alpha_j)$,

[‡] This is to avoid the degeneracy between negative amplitudes (after taking the logarithm) with positive phases and positive amplitudes with opposite phases.

$\alpha_1 =$ $-3\alpha_7 + 2\alpha_{11} + \pi$	$\alpha_2 =$ $5\alpha_7 - 3\alpha_{11} + \pi$	$\alpha_3 =$ $2\alpha_7 - \alpha_{11} + \pi$	$\alpha_4 =$ $-\alpha_7 + \alpha_{11} + \pi$	$\alpha_5 =$ $-4\alpha_7 + 3\alpha_{11}$	$\alpha_6 =$ $-4\alpha_7 + 2\alpha_{11}$	α_7
$\alpha_8 =$ $-2\alpha_7 + 2\alpha_{11}$	$\alpha_9 =$ $6\alpha_7 - 3\alpha_{11} + \pi$	$\alpha_{10} =$ $3\alpha_7 - \alpha_{11}$	α_{11}	$\alpha_{12} =$ $-3\alpha_7 + 3\alpha_{11} + \pi$	$\alpha_{13} =$ $5\alpha_7 - 2\alpha_{11}$	$\alpha_{14} =$ $2\alpha_7$
$\alpha_{15} =$ $-\alpha_7 + 2\alpha_{11} + \pi$	$\alpha_{16} =$ $-4\alpha_7 + 4\alpha_{11}$	$\alpha_{17} =$ $4\alpha_7 - \alpha_{11} + \pi$	$\alpha_{18} =$ $\alpha_7 + \alpha_{11}$	$\alpha_{19} =$ $-2\alpha_7 + 3\alpha_{11}$	$\alpha_{20} =$ $6\alpha_7 - 2\alpha_{11}$	$\alpha_{21} =$ $3\alpha_7$
$\alpha_{22} =$ $2\alpha_{11}$	$\alpha_{23} =$ $-3\alpha_7 + 4\alpha_{11} + \pi$	$\alpha_{24} =$ $5\alpha_7 - \alpha_{11} + \pi$	$\alpha_{25} =$ $2\alpha_7 + \alpha_{11}$	$\alpha_{26} =$ $-\alpha_7 + 3\alpha_{11} + \pi$	$\alpha_{27} =$ $-4\alpha_7 + 5\alpha_{11}$	$\alpha_{28} =$ $4\alpha_7$
$\alpha_{29} =$ $\alpha_7 + 2\alpha_{11}$	$\alpha_{30} =$ $-2\alpha_7 + 4\alpha_{11}$	$\alpha_{31} =$ $6\alpha_7 - \alpha_{11} + \pi$	$\alpha_{32} =$ $3\alpha_7 + \alpha_{11}$	$\alpha_{33} =$ $3\alpha_{11}$	$\alpha_{34} =$ $-3\alpha_7 + 5\alpha_{11} + \pi$	$\alpha_{35} =$ $5\alpha_7$
$\alpha_{36} =$ $2\alpha_7 + 2\alpha_{11}$	$\alpha_{37} =$ $-\alpha_7 + 4\alpha_{11} + \pi$	$\alpha_{38} =$ $-4\alpha_7 + 6\alpha_{11}$	$\alpha_{39} =$ $4\alpha_7 + \alpha_{11}$	$\alpha_{40} =$ $\alpha_7 + 3\alpha_{11}$	$\alpha_{41} =$ $-2\alpha_7 + 5\alpha_{11}$	$\alpha_{42} =$ $6\alpha_7$
$\alpha_{43} =$ $3\alpha_7 + 2\alpha_{11}$	$\alpha_{44} =$ $4\alpha_{11}$	$\alpha_{45} =$ $-3\alpha_7 + 6\alpha_{11} + \pi$	$\alpha_{46} =$ $5\alpha_7 + \alpha_{11}$	$\alpha_{47} =$ $2\alpha_7 + 3\alpha_{11}$	$\alpha_{48} =$ $-\alpha_7 + 5\alpha_{11} + \pi$	$\alpha_{49} =$ $7\alpha_7$

Table 1. The predicted phases from the harmonic relation for parent wavenumber 7 and 11 for Fig.1 and 2. The terms with odd number of complex conjugate u_k give rise to an extra phase shift by π , apart from the harmonic relation. The spawned modes that have combinations from the parent wavenumbers (with lower orders) will grow, with phases following the same harmonic relation. Those suppressed are modes which need high orders of combinations from wavenumbers of the parent modes (those in frames, e.g. $k = 13$ and 38).

$$u_k = -\frac{1}{2i} \sum_j A_j \lambda_j e^{i\alpha_j} \delta^D(\lambda_j - k) = -\frac{A_k \lambda_k}{2i} e^{i\alpha_k} = \frac{A_k \lambda_k}{2} e^{i(\pi/2 + \alpha_k)}, \quad (42)$$

and u_{-k} is simply its complex conjugate.

Equation (41) and (42) provide us the insight into mode spawning and mode merging in gravitational clustering. The Dirac-delta functions dictate the spawning of Fourier modes, both the amplitudes and phases. If, for any Fourier mode k , there is only one combination from the parent modes, its phase α_k shall not change and the amplitude grow steadily with $b(t)^n$ (according to the order of this combination). If, on the other hand, there is more than one set of combination for wavenumber k [cf Eq. (24)], they will interact so that the phase α_k will be changed accordingly.

To be more specific, in our case of two cosine functions in $\Phi_0(q)$ (in Fig.1 and 2) from which only u_{λ_a} and u_{λ_b} exist ($\lambda_b > \lambda_a$), we can write down explicitly what constitutes the Fourier mode of wavenumber k : the first term in Eq. (41) is simply $A_k \lambda_k k b e^{i\alpha_k} / 2$. The second term has all the combinations of any two from λ_a and λ_b in the Dirac-delta functions: $2\lambda_a$, $2\lambda_b$, $\lambda_a + \lambda_b$ and $\lambda_a - \lambda_b$ so that

$$\begin{aligned} & \frac{(-ikb)^2}{2!} \sum_{k_1, k_2} u_{k_1} u_{k_2} \delta^D[k - (k_1 + k_2)] \\ &= \frac{k^2 b^2 e^{i\pi}}{2} \left[\frac{A_{\lambda_a} A_{\lambda_b} \lambda_a \lambda_b}{4} e^{i(\alpha_{\lambda_a} + \alpha_{\lambda_b} + \pi)} \delta^D(k - \lambda_a - \lambda_b) + \frac{A_{\lambda_a} A_{\lambda_b} \lambda_a \lambda_b}{4} e^{i(\alpha_{\lambda_b} - \alpha_{\lambda_a})} \delta^D(k + \lambda_a - \lambda_b) \right. \\ &+ \left. \frac{A_{\lambda_a}^2 \lambda_a^2}{4} e^{i(2\alpha_{\lambda_a} + \pi)} \delta^D(k - 2\lambda_a) + \frac{A_{\lambda_b}^2 \lambda_b^2}{4} e^{i(2\alpha_{\lambda_b} + \pi)} \delta^D(k - 2\lambda_b) \right]. \end{aligned} \quad (43)$$

If the Φ_0 has more than two cosine functions, the second term of Eq. (41) then shall have all the combinations of any 2 from Φ_0 . The third term involves combinations of any 3 from λ_a and λ_b , i.e. $3\lambda_a$, $3\lambda_b$, $2\lambda_a \pm \lambda_b$, $\lambda_a \pm 2\lambda_b$. It is also worth noting that unless the higher-order terms exist (i.e. $\delta^D[k - (k_1 + k_2 + k_3)] = 1$), the phases of the Fourier modes are fixed and the amplitudes grow with b^n .

For the interactive parent modes in Eq.(37) (Fig. 3), where $\lambda_3 = 2\lambda_1$, the second term of Eq.(41) has one Dirac-delta function involving $\lambda_3 + \lambda_2$ whereas in the third term there is another involving $2\lambda_1 + \lambda_2$. The resultant phase of this wavenumber depends on the amplitudes of the terms involving the two Dirac-delta functions.

Note that for wavenumber $k = \lambda_b - \lambda_a$ of Eq.(43) the phase is $\alpha_{\lambda_b} - \alpha_{\lambda_a} + \pi$. This extra phase shift by π is due to odd number of complex conjugate of u_k in Eq. (41).

In Table 1 we show the predicted phases of the spawned Fourier modes from the parent modes for Fig. 1 and 2. The wavenumbers of the parent modes are 7 and 11. The spawned modes that have the combination of the parent wavenumber (with lower orders) will grow following the wavenumber-phase harmonic relation. Those which are suppressed (or have not grown before shell crossing) are modes which need high orders of combinations in wavenumbers or which have no exact

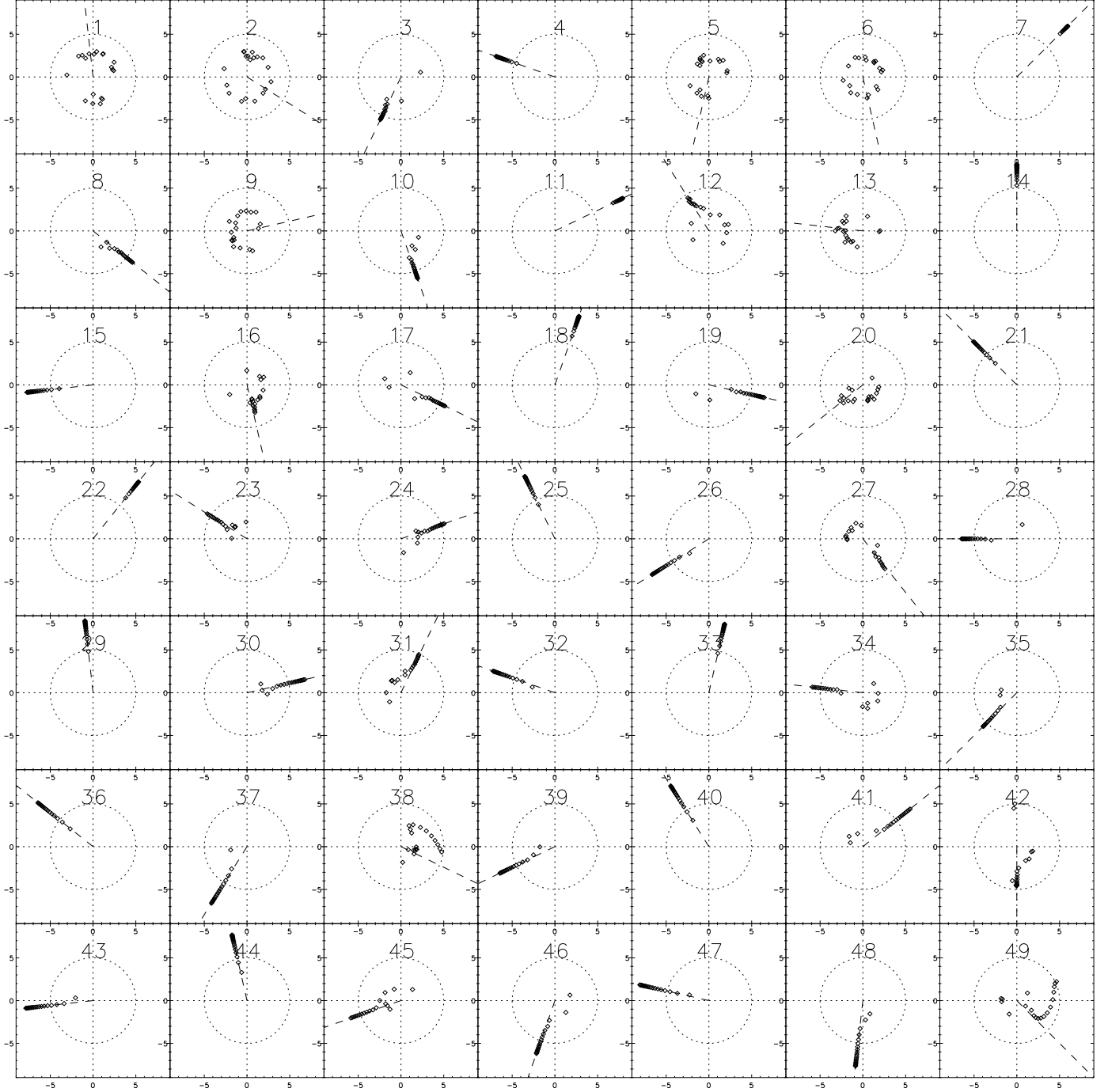


Figure 2. The amplitude and phase evolution (wavenumber $k = 1 - 49$) of 1D ZA simulation with $\Phi_0 = -\cos(7q + \pi/4) - \cos(11q + \pi/7)$. In each panel the amplitude ($\times 10^9$) is shown in logarithmic scale by the distance of each symbol to the origin, and the phase by the angle against the positive x axis. Thus the dotted circle in each panel indicates amplitude with 10^{-4} . The dash lines indicate the predicted phases according to Table 1: the wavenumber-phase harmonic relation.

combination. The phase of wavenumber 24: α_{24} , for example, can have combinations of $5\alpha_7 - \alpha_{11}$ or $-6\alpha_7 + 6\alpha_{11}$. The former is of the 6th order and the latter is the 12th order in terms of $b(t)$ series in Eq.(41). The low-order combination of wavenumbers prevails at the early stage and if it is dominant in amplitude, the other combinations will have little influence. When the parent modes are “interactive”, the phase sets out with a value from lower-order combination. In Fig. 3 we have 3 parent modes $\lambda_1 = 7$, $\lambda_2 = 11$ and $\lambda_3 = 14$. The phase of mode $k = 18$ is spawned from $\alpha_7 + \alpha_{11}$ in the beginning and $3\alpha_7 + \alpha_{11} - \alpha_{14}$ at later stage. It is only at very later stage of evolution that the 5th order can catch up with the 2nd order (see Fig. 3).

Having such rules in mind, one can clearly see why the parent low-frequency modes (and their phases) have decisive influence on the mode coupling. As shown in Chiang & Coles (2000), convergence of phase difference $D_k = \phi_{k+1} - \phi_k$ at high

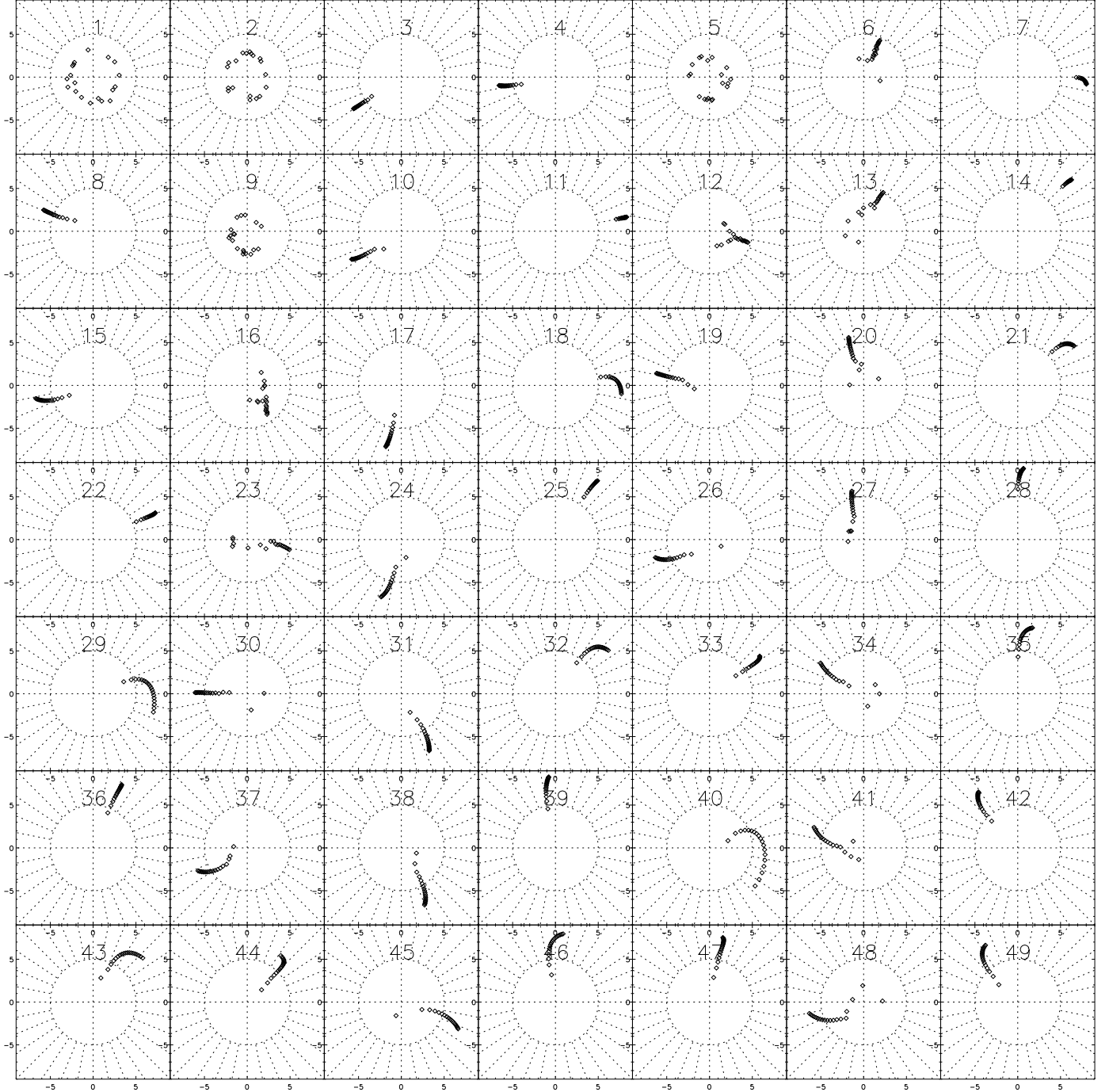


Figure 3. The amplitude and phase evolution of 1D ZA simulation with $\Phi_0 = -\cos(7q) - \cos(11q + \pi/16) - \cos(14q + \pi/4)$. As in Fig. 1 the radial dotted lines are angles with an increment of $\pi/16$ to show that phases align with angles of multiple of $\pi/16$. One can see now, with the extra parent mode $\lambda_3 = 14$ interacting, the phases are shifted considerably. Note also that in this case, the wavenumber-phase harmonic relation is broken.

k is related to the location of the highest density peak. The wavenumbers of parent lowest-frequency mode ($k = 1$) can easily be added (or subtracted) to form precisely the spawned wavenumbers, particularly for high-frequency modes, so the phase of the lowest k mode would inevitably take part in most of the high k mode spawning. Hence the increment in phases (i.e. D_k) along k axis would be the phase from the lowest frequency mode ($k = 1$).

Note also that for more generic situations where all modes in Φ_0 have non-zero amplitudes, they are definitely “interactive”, in particular with the presence of fundamental mode $k = 1$. Therefore, the evolution of amplitudes and phases shall have a complicated picture with mode merging with changing of Fourier amplitudes and phases.

5 DISCUSSIONS

In this paper, we use 1D ZA to illustrate some non-linear effects induced by gravitational clustering: mode spawning and mode coupling. We first demonstrate the onset of non-linearity by expanding the density contrast in terms of power series of $b(t)$. The second-order of such expansion reflects quadratic density fields, from which modes are spawned with phases following a special wavenumber-phase harmonic relation. We have also illustrated with toy models that the widely-used statistic, bispectrum, can only pick up the quadratic phase coupling and is blind to cubic and higher-order phase coupling. We further perform direct 1D ZA simulations in order to demonstrate these effects entering non-linear regime. The wavenumber-phase harmonic relation holds as long as the wavenumbers of parent modes are not “interactive”, as shown in Fig. 1 and 2. The complexity of Fourier amplitude and phase evolution comes from the continuous interactions between modes and their merging and coupling with the spawned modes.

Recently it is also claimed that bispectrum measures phase correlations (Komatsu et al. 2003), which is partially correct. We have demonstrated with toy models that bispectrum measures only *quadratic* phase coupling under the condition that the wavenumber-phase harmonic relation holds, as pointed out in details in Watts & Coles (2002). Upon using bispectrum as a test of non-Gaussianity, a quadratic field such as the form $\delta(\mathbf{x}) + \epsilon\delta^2(\mathbf{x})$ could give a zero bispectrum due to the interaction between the spawned modes in $\epsilon\delta^2(\mathbf{x})$ with the parent ones in $\delta(\mathbf{x})$, hence resulting in a false signature of Gaussianity. Moreover, the blindness of bispectrum to higher-order phase coupling indicates that a complete hierarchy of polyspectra is required to fully characterize the statistical properties of a fluctuation field.

The initial power spectral index decides the clustering morphology, which is closely related to Fourier phases (Chiang 2001). It is therefore interesting to examine the link between Gaussian random fields with different initial power spectral index, the only available information, and evolved morphology with information encoded in phases rather than in amplitudes. The 1D ZA simulations in this paper can be considered as from initial white noise power spectrum with spectral index $n = 0$ (as the coefficients of cosine functions in the velocity potential are all unity). It is clear that mode spawning is independent of amplitudes of the parent modes, but mode merging and coupling is rather dependent on the amplitudes of spawned modes, which are originated from parent ones. How the information is transferred from Fourier amplitudes to different phase coupling configurations will be examined in the next paper.

ACKNOWLEDGMENTS

This paper was supported in part by Danmarks Grundforskningsfond through its support for the establishment of the Theoretical Astrophysics Center. The author thanks Peter Coles for useful suggestions and Pavel Naselsky for discussions.

REFERENCES

- Bardeen J.M., Bond J.R., Kaiser N., Szalay A.S., 1986, ApJ, 304, 15
- Bernardeau F., 1992, ApJ, 392, 1
- Bernardeau F., Colombi S., Gaztanaga E., Scoccimarro R., 2002, Phys. Rep., 367, 1
- Buchert T., 1992, MNRAS, 254, 729
- Chiang L.-Y., 2001, MNRAS, 325, 405
- Chiang L.-Y., Coles P., 2000, MNRAS, 311, 809
- Chiang L.-Y., Coles P., Naselsky P.D., 2002, MNRAS, 337, 488
- Chiang L.-Y., Naselsky P.D., Coles P., 2002, ApJL submitted (astro-ph/0208235)
- Chiang L.-Y., Naselsky P.D., Verkhodanov O.V., Way M.J., 2003, ApJ, 590, L65
- Coles P., Chiang L.-Y., 2000, nat, 406, 376
- Coles P., Chiang L.-Y., 2001, in Banday A.J., Zaroubi S., Bartelmann M., eds., Proc. of the MPA/ESO/MPE Workshop “Mining the Sky” held at Garching, Germany, July 31 - August 4, 2000, Springer-Verlag series “ESO Astrophysics Symposia” (astro-ph/0010521)
- Coles P., Barrow J.D., 1987, MNRAS, 228, 407
- Goroff M. H., Grinstein B., Rey S. J., M.B Wise., 1986, ApJ, 311, 6
- Hikage C., Matsubara T., Suto Y., 2003, ApJ submitted (astro-ph/0308472)
- Hivon E., Bouchet F.R., Colombi S., Juszkiewicz R., 1995, A&A, 298, 643
- Jain B., Bertschinger E., 1998, ApJ, 509, 517
- Komatsu E. et al., 2003, ApJ submitted (astro-ph/0203223)
- Matarrese S., Verde L., Heavens A.F., 1997, MNRAS, 290, 651
- Matsubara T., 2003, ApJL accepted (astro-ph/0303278)
- Padmanabhan T., 1993, Structure Formation in the Universe, Cambridge University Press, Cambridge, UK
- Peeble P.J.E., 1980, The Large-scale structure of the Universe, Princeton University Press
- Ryden B., Gramann M., 1991, ApJ, 383, 33
- Scoccimarro R., 1997, ApJ, 487, 1
- Scoccimarro R., Couchman H.M.P., Frieman J.A., 1999, ApJ, 517, 531
- Scoccimarro R., Colombi S., Fry J.N., Frieman J.A., Hivon E., Melott A.L., 1998, ApJ, 496, 586
- Scherrer R.J., Melott A.L., Shandarin S.F., 1991, ApJ, 377, 29

- Soda J., Suto Y., 1992, ApJ, 396, 379
Stirling A.J., Peacock J.A., 1996, MNRAS, 283, L99
Verde L., Wang L., Heavens A.F., Kamionkowski M., 2000, MNRAS, 313, 141
Watts P.I.R., Coles P., 2002, MNRAS, 338, 806
Watts P.I.R., Coles P., Melott A., 2003, ApJ, 589, L61
Zel'dovich Ya.B., 1970, A&A, 5, 84